EVIDENCE OF EARLY PALAEOZOIC CONTINENTAL RIFTING FROM MAFIC METAVOLCANICS OF SOUTHERN PELORITANI MOUNTAINS (NORTH-EASTERN SICILY, ITALY)

Rosolino Cirrincione*, Patrizia Fiannacca, Antonino Lo Giudice**** and **Antonino Pezzino****

***** *Dipartimento di Scienze della Terra, Università della Calabria, I-87036 Arcavacata di Rende, Cosenza, Italy (Corresponding author, e-mail: cirrincione@unical.it).*

****** *Dipartimento di Scienze Geologiche, Università di Catania, Corso Italia 55, I-95129 Catania, Italy.*

Keywords: *Metabasites, P-MORB affinity, continental break-up, Cambro-Ordovician, Peloritani Mountain Belt.*

ABSTRACT

Pre-Hercynian magmatic rocks are widespread in the Palaeozoic basement of the Peloritani Mountain Belt. The metabasites of the Mongiuffi-Melia area (SE Peloritani) represent the largest magmatic products of Early Palaeozoic. These rocks occur as mafic lava flows and metavolcanoclastites often preserving relict igneous textures. They were weakly metamorphosed during the Hercynian orogenesis and show sub-greenschist metamorphic assemblages overprinting the original igneous parageneses. The geochemical features of these rocks indicate an alkali basaltic composition and a within-plate to P-MORB affinity. Basaltic protoliths of metabasites were produced by partial melting of variably enriched mantle sources and experienced fractionation and little crustal contamination during their ascent. Overall data are consistent with a geodynamic environment related to an early stage of tectonically dominated continental rifting. These metabasites represent the only evidences of a Cambro-Ordovician extensional event in the Peloritani domain of the former Alboran microplate. Their features are consistent with a possible location of this terrane at the south-western termination of the South Armorican Ocean during the Early Palaeozoic.

INTRODUCTION

The pre-Hercynian terranes of the peri-Mediterranean area are mainly exposed as basement areas affected by Hercynian and/or Alpine medium to high grade metamorphism. The occurrence of very low-grade mono-metamorphic Hercynian terranes provides important clues for the geodynamic interpretation of the Early Palaeozoic period in the Central Mediterranean area. Generation of Cambro-Ordovician oceanic crust (Rheic Ocean) has been reported from several basement areas (von Raumer et al., 2002; Schaltegger et al., 2002), however only stages of initial rifting are indicated for the terranes located eastward respect to Avalonia, before its separation from the other peri-Gondwanan microcontinents (Stampfli and Borel, 2002; von Raumer et al., 2003).

Evidences of continental break-up, reported from different parts of the Hercynian Europe (von Raumer et al., 1990; Pin and Marini, 1993; Capelli et al., 1994, von Raumer et al., 2002), consist of mafic-ultramafic complexes or bimodal associations of felsic and mafic meta-igneous rocks with alkaline affinity.

Alkaline metabasites of Cambro-Ordovician age crop out in the Mongiuffi-Melia (MM) area, within the Lower Domain of the Peloritani Belt (north-eastern Sicily). These metavolcanic products seem to represent the only available evidence for the reconstruction of the Lower Palaeozoic extensional events in this sector of the former Alboran microplate (Andrieux et al., 1971).

The very-low grade Hercynian metamorphism commonly preserved primary volcanic textures thus allowing for protolith identification. At the same time, most geochemical features have been retained, permitting some petrological considerations.

The present study provides petrographical, geochemical and Nd-isotope data for the Mongiuffi-Melia metabasites in order to determine the origin and the evolution of their magmatic protoliths and put constraints on the palaeogeographic environment at the time of their emplacement.

GEOLOGICAL SETTING

The Peloritani Mountain Belt is located in north-eastern Sicily. It forms the southern part of the Calabrian-Peloritani Arc, a segment of the Variscan Belt that represents the connection between the Southern Apennine Chain and the Maghrebid Chain (Fig. 1). The evolution and geodynamic significance of the Calabrian-Peloritani Arc are still the subject of contrasting interpretations, due to its involvement in both Hercynian and Alpine orogeneses. The Peloritani Range is composed of a nappe pile consisting of Hercynian basement rocks whose metamorphic grade increases northward and of fragments of Mesozoic-Cenozoic covers. This nappe pile can be subdivided into two domains, namely Lower and Upper Domain, characterised by different tectonic-metamorphic histories (Atzori et al., 1994; Cirrincione and Pezzino, 1994). The Lower domain is exposed in the southern part of the Peloritani Belt and consists of three tectonic slices made up of very low- to low-grade metamorphic sequences and non-metamorphosed Mesozoic-Cenozoic cover rocks. The metamorphic characteristics of these tectonic units have been previously described (Atzori and Ferla, 1979; Pezzino 1982). The Upper Domain, in the north-eastern part of the belt, consists of two tectonic units mainly made up of low- to high-grade Hercynian metamorphic rocks, characterized by an Alpine metamorphic overprint.

Metapelites, quartzite schists and minor marbles and metabasites compose the three tectonic units forming the Lower Domain. In the Mongiuffi-Melia area (Fig. 2a) a metavolcanic formation composed of metabasalts and metavolcaniclastic rocks crops out at the base of the intermediate tectonic unit (Taormina Unit; Atzori et al., 2001 and reference therein). The metabasalts are the subject of the present study. The underlying metapelites, in stratigraphic contact with the volcanic succession, contain acritarchs (Cambrian-Ordovician transition, Majesté-Menjoulas et al., 1986; Bouillin et al., 1987), thus suggesting a likely Cambro-Or-

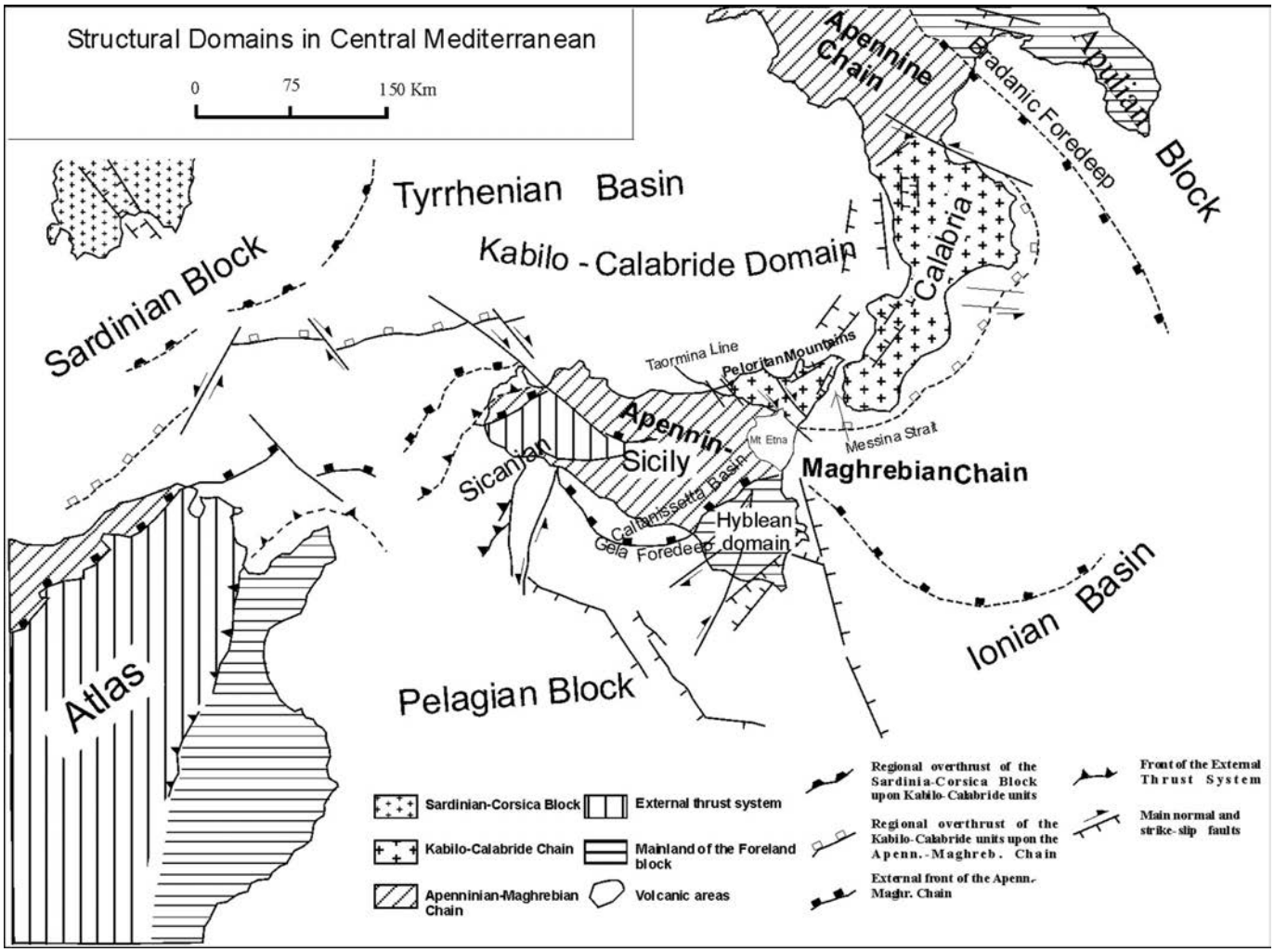

Fig. 1 - Simplified structural map of the Central Mediterranean area (modified from Lentini et al., 1995).

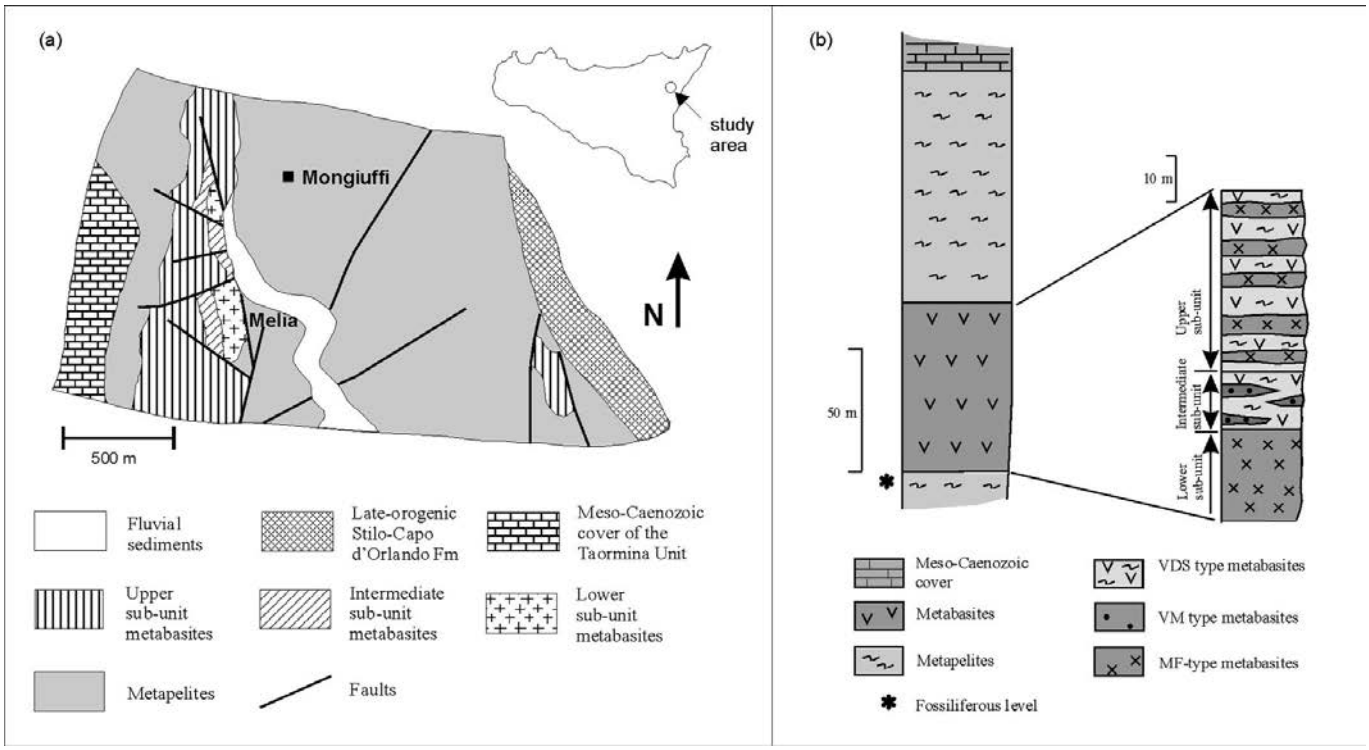

Fig. 2 - (a) simplified geologic map (modified from Cirrincione et al., 1999); (b) geological section of the Mongiuffi-Melia area. (MF: massive metabasite; VM: vesicular metabasite; VDS: metavolcaniclastic rock).

dovician age. According to Acquafredda et al. (1994), these metabasites represent the oldest eruptive products of the Palaeozoic sequence of the Peloritani Mountain Belt.

SECTIONS AND FIELD OBSERVATIONS

The metavolcanics are green to greenish-violet in colour, fine-grained and have massive to foliated structure. Three rock types can be distinguished:

1) Massive dark green metabasite (MF), exhibiting a poorly developed metamorphic foliation. It likely represents the metamorphic product of original massive lava flows.
2) Poorly foliated vesicular metabasite (VM) of colour from violet to green-violet. The presence of vesicles suggests that this rock type represents the metamorphic product of original vesicular lava flows. Locally calcite-filled amygdales, 0.5-1 cm in size, have been produced by secondary filling of magmatic vesicles.
3) Metavolcaniclastic rock types (VDS) represent metamorphic products of original pyroclastic material, preserving an original volcaniclastic layering of variable thickness (from few centimetres to 4-5 m). They are characterised by a marked foliation and variable colours, from grey-green to violet.

The metavolcanic succession is composed of: 1) a 20 m thick basal sub-unit made up of MF-type metabasite; 2) a 15 m thick intermediate sub-unit mainly consisting of alternating levels of VDS and VM-type metabasites; 3) a 45 m thick upper sub-unit mainly composed of VDS with interbedded MF-type metabasite lenticular bodies (Fig. 2b).

PETROGRAPHY AND METAMORPHISM

Most samples show sub-greenschist-facies mineral assemblages. In MF- and VM-metabasites, relics of magmatic textures (e.g. porphyritic textures and flow fabrics) are often present. Phenocrysts were composed of mafic minerals and plagioclase, now replaced by chlorite + calcite + quartz + epidote aggregates and albite crystals, respectively. The microcrystalline groundmass, showing intergranular to intersertal texture, is now mainly containing chlorite and albite. The other minerals of the groundmass include epidote, calcite, pumpellyite, prehnite, iron oxides, quartz, white mica; actinolite is sporadically present.

Occurrence of vesicles and the association with volcaniclastic products suggest a shallow-water depositional environment. The metamorphic evolution of these rocks can be ascribed to two stages (Cirrincione et al., 1999): 1) a first stage produced the main foliation S_1 and generated sub-greenschist facies assemblages: the VM-type metabasites are characterised by a prehnite-bearing assemblage, while the MF-type metabasites are either pumpellyite-bearing or actinolite bearing; 2) the second stage produced the S_2 foliation crenulation cleavage, mainly evident in the rocks of VDS type. During the second stage the introduction of a CO_2-rich fluid played a fundamental role stabilizing the "Cal + Chl" assemblage at the expense of the previous sub-greenschist facies assemblages.

ANALYTICAL METHODS

Major and trace elements of fourteen representative samples from the MM area, (excluding metavolcaniclastic products), were measured by inductively coupled plasma atomic emission spectrometry (ICP-AES) and inductively coupled plasma mass spectrometry (ICP-MS) at the Nancy CRPG laboratory (CNRS). Details of the analytical procedure and detection limits are described by Carignan et al. (2001). Two selected samples were analysed for Nd isotope ratios at the Nancy CRPG laboratory (CNRS). Sm and Nd concentrations were determined by isotope dilution. Isotopic compositions were measured using a Finnigan MAT 262 mass spectrometer. Measured $^{143}Nd/^{144}Nd$ ratios were normalised to $^{146}Nd/^{144}Nd = 0.7219$. Repeated measurements of CNRS internal J-M standard yielded an average value of $^{143}Nd/^{144}Nd = 0.511089 \pm 38$ (2σ) during the period of analysis corresponding to a La Jolla value of 0.511827.

GEOCHEMISTRY

Major and trace element data of the analysed representative samples of Mongiuffi-Melia metabasites (MF and VM types) are reported in Table 1.

MM metabasites have SiO_2 contents in the range 42.7-49.6 wt.% (recalculated on anhydrous basis). In the Harker diagrams (not shown) MM samples are scattered and no clear evolutionary trend can be recognised. MF-type samples from the lower sub-unit generally have higher TiO_2, Al_2O_3, Zr, La, Y and lower Ni, Cr (and LOI) contents than types coming from the two upper sub-units. On the contrary samples from the upper sub-unit have the highest abundances of MgO (10.38-12.03 wt.%), Co (48-53 ppm), Ni (226-246 ppm) and Cr (561-633 ppm). The metabasites of the intermediate sub-unit show intermediate geochemical characteristics compared with the rocks of the other two sub-units, except for the relatively low contents of TiO_2 and Fe_2O_{3tot}.

The abundances of selected compatible and incompatible elements have been plotted against Zr employed as a fractionation index (Fig. 3). Despite some scattering the diagrams show that TiO_2, Fe_2O_{3tot}, Al_2O_3, Nb, Y, La abundances tend to increase with increasing Zr content, while MgO, CaO, Na_2O, Cr, Ni show negative correlation. The observed trends are explainable in terms of fractional crystallization of olivine + clinopyroxene ± spinel. No clear correlation is recognizable for K_2O, likely reflecting some post-magmatic mobilization.

All the MM metabasites show alkaline affinity, as already recognized by Ferla (1978). They plot in the field of alkali basalts in the Nb/Y vs. Zr diagram (Fig. 4a), which also shows the more evolved nature of the samples from the lower sub-unit. On the contrary, samples from the two upper sub-units plot close to the field of tholeiitic basalts and show a more primitive character. In the TiO_2-V diagram (Fig. 4b) it is possible to evidence the general high-Ti nature of all the metabasite samples. In particular the high Ti contents may be explained in terms of different processes which could have interacted at various degrees (e.g source features, small amount of partial melting, etc.; Shervais, 1982).

MM metabasites plot within the field of within-plate basalts in the Ti-Zr-Y diagram (Pearce and Cann, 1973) whereas in the Hf–Th-Ta diagram (Wood, 1979) it is possible to observe that the samples from the lower massive sub-unit plot within the intraplate basalts field and the samples from the intermediate and upper sub-units straddle the limit among the intraplate basalts field and the E-MORB field (Fig. 5).

Table 1 - Major and trace element composition of the Mongiuffi Melia metabasites

	Lower subunit							Intermediate subunit					Upper subunit	
	MM1	MM 2	MM 3	MM 4	MM 5	MM 6	MM 9	MM 20	MM 21	MM 23	MM 24	MM 29	MM 46	MM 47
sample type	MF	MF	MF	MF	MF	MF	MF	VM	VM	VM	MF	MF	MF	MF
Major elements (wt. %)														
SiO_2	41.79	40.53	39.41	39.5	42.88	43.08	44.28	41.98	37.07	40.82	45.79	40.23	42.91	43.15
TiO_2	2.69	2.72	2.68	3.07	2.73	2.87	2.7	1.51	1.38	1.47	1.76	1.73	2.14	1.89
Al_2O_3	16.89	16.82	17.14	18.24	17.4	17.08	16.4	14.16	12.49	13.79	15.03	13.64	14.54	13.27
Fe_2O_3	12.53	12.95	15.42	14.78	11.72	12.83	12.35	9.71	9.82	9.39	9.31	11.12	14.2	12.32
MnO	0.18	0.12	0.16	0.12	0.19	0.14	0.15	0.06	0.07	0.05	0.12	0.15	0.09	0.11
MgO	6.45	4.21	7.19	6.77	6.33	6.48	6.29	2.48	2.71	2.82	8.59	10.42	12.03	10.38
CaO	6.64	8.29	5.33	4.29	6.1	5.55	5.54	12.77	16.39	13.21	6.31	9.17	3.71	6.89
Na_2O	4.83	3.81	4.25	0.13	4.97	4.98	5.07	6.23	5.65	5.63	4.91	2.23	2.07	2.26
K_2O	0.35	2.32	0.31	2.04	0.38	0.28	0.15	0.69	0.5	1.21	0.15	0.03	0.01	0.01
P_2O_5	0.52	0.5	0.47	0.57	0.56	0.51	0.53	0.37	0.33	0.4	0.38	0.3	0.35	0.37
LOI	7.08	7.59	7.57	7.33	6.3	6.12	6.49	9.92	13.51	11.08	7.32	10.87	7.84	9.33
Trace elements (ppm)														
V	236	246	228	304	228	239	231	204	182	166	216	228	244	226
Cr	21.6	23,00	33.6	26.3	22.2	23.3	21,00	335,00	331,00	302,00	381,00	364,00	633	561
Co	38.4	42.7	41.4	40.5	37.6	35.5	34.2	26.5	29.2	29.4	42.2	42.2	53	48
Ni	33.2	41.4	43.2	33.5	28.4	30.3	26.8	84.2	95,00	114,00	133,00	125,00	246	226
Rb	9.4	55.87	8.73	46.49	11.96	9.02	5.54	18.46	13.87	32.14	4.22	1.4	0.421	0.56
Sr	257	351	342	117	401	276	267	265	212	216	146	254	53.3	148
Y	30.1	31.3	28.7	32.4	30.3	31.5	27.5	19.3	19.9	24.4	24.1	20.5	23.2	18.9
Zr	224	230	225	250	221	238	220	167	155	158	187	194	133	116
Nb	41.16	42.31	40.93	46.44	40.62	42.81	39.78	18.29	17.53	18.36	20.59	21.74	17.77	15.69
Ba	109	531	171	529	116	85	64	231	183	240	56	28	11	27
La	38.13	35.41	36.03	37.24	33.55	39.1	33.68	17.93	20.57	26.59	19.29	19.85	18.34	13.52
Ce	74.5	71.03	71.12	77.08	68.7	76.79	66.58	37.1	40.51	54.9	41.64	40.18	41.44	31.15
Pr	8.21	8.04	7.88	8.76	7.56	8.44	7.47	4.24	4.56	6.19	4.77	4.48	5.08	3.9
Nd	34.51	32.69	33.14	37.23	30.61	34.93	30.52	17.24	20.06	25.98	20.41	19.62	23	18.04
Sm	7.12	7.07	7.3	8.18	7.15	7.58	6.57	3.96	4.45	5.66	4.81	4.21	5.58	4.44
Eu	2.37	2.39	2.37	2.69	2.22	2.48	2.14	1.39	1.35	1.76	1.57	1.57	2.02	1.67
Gd	6.71	6.8	6.83	7.84	6.95	7.61	6.2	4.16	4.32	5.6	4.77	4.34	5.38	4.49
Tb	0.97	1.03	1.00	1.09	0.95	1.07	0.91	0.63	0.62	0.81	0.77	0.63	0.8	0.65
Dy	5.61	5.79	5.64	6.15	5.67	6,00	5.07	3.65	3.6	4.62	4.31	3.82	4.46	3.68
Ho	1.13	1.16	1.14	1.33	1.12	1.27	1.04	0.79	0.75	0.95	0.9	0.79	0.88	0.76
Er	2.65	2.73	2.8	3.07	2.69	2.8	2.4	1.81	1.85	2.29	2.07	1.93	2.01	1.67
Tm	0.4	0.4	0.4	0.46	0.4	0.41	0.36	0.29	0.27	0.35	0.32	0.28	0.29	0.26
Yb	2.4	2.42	2.54	2.77	2.52	2.42	2.26	1.71	1.59	2.05	2.05	1.82	1.77	1.44
Lu	0.36	0.36	0.35	0.41	0.36	0.36	0.35	0.25	0.27	0.32	0.29	0.25	0.24	0.21
Hf	4.97	5.04	5.05	5.82	5.15	5.37	4.71	3.78	3.46	3.61	4.13	4.37	3.11	2.72
Ta	2.63	2.7	2.66	3.06	2.64	2.84	2.55	1.33	1.23	1.31	1.44	1.53	1.19	1.04
Th	4.88	4.86	5.07	5.7	4.84	5.1	4.53	3.22	2.94	3.05	3.47	3.72	2.29	1.99
U	1.04	0.98	1.3	1.3	0.99	1.05	0.96	0.54	0.57	0.51	0.81	0.87	0.52	0.51
Zr/Nb	5.44	5.44	5.5	5.38	5.44	5.56	5.53	9.13	8.84	8.61	9.08	8.92	7.48	7.39
Zr/Y	7.44	7.35	7.84	7.72	7.29	7.56	8,00	8.65	7.79	6.48	7.76	9.46	5.73	6.14
Y/Nb	0.73	0.74	0.70	0.7	0.75	0.74	0.69	1.06	1.14	1.33	1.17	0.94	1.31	1.2
La/Nb	0.93	0.84	0.88	0.8	0.83	0.91	0.85	0.98	1.17	1.45	0.94	0.91	1.03	0.86

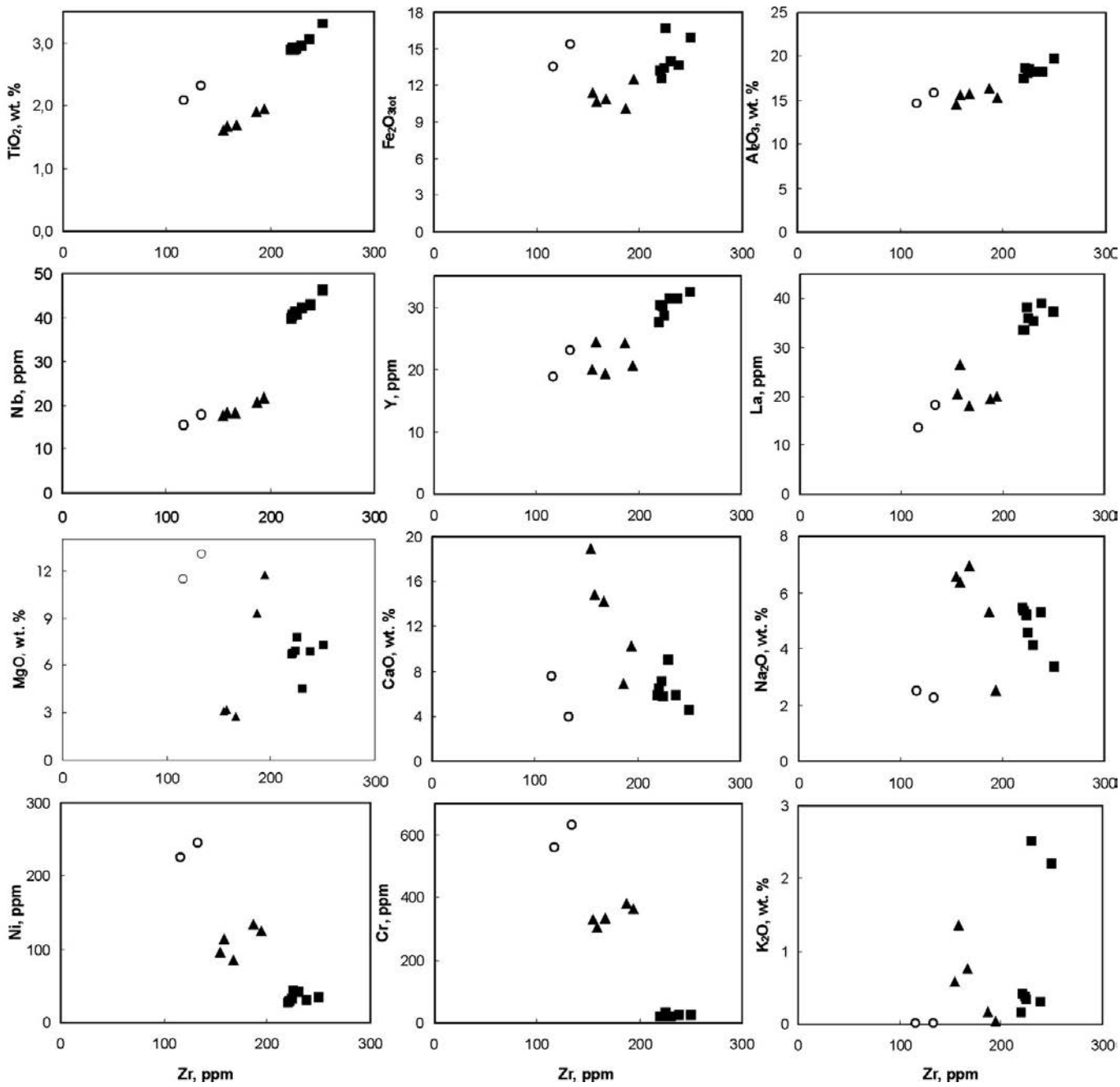

Fig. 3 - Major, minor and trace elements plotted against Zr. Squares = lower sub-unit samples; triangles = intermediate sub-unit samples ; circles = upper sub-unit samples.

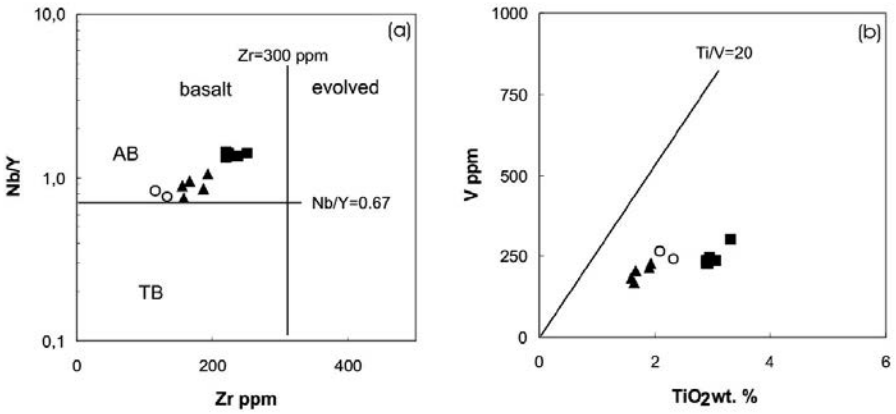

Fig. 4 - Chemical discrimination of MM metabasites; references after Floyd et al., 2000. (a) Nb/Y versus Zr diagram (AB = alkaline basalts; TB = tholeiitic basalts); (b) V-TiO_2 diagram. Symbols as in Fig. 3.

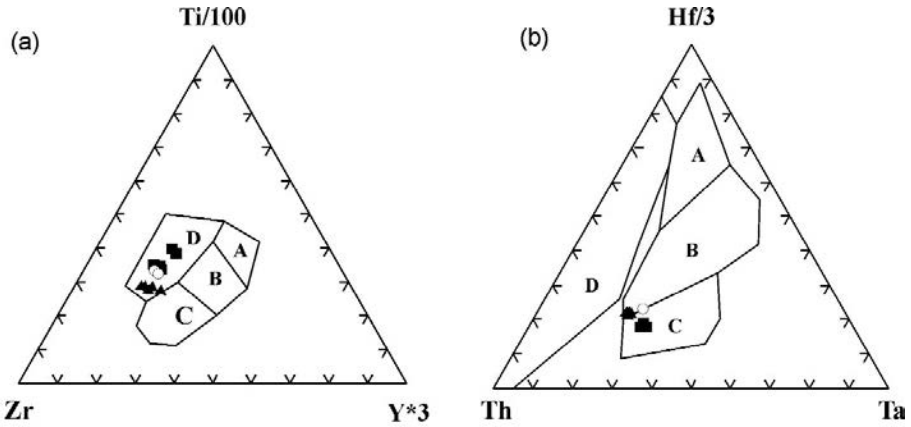

Fig. 5 - Discrimination diagrams for the MM metabasites. (a) Ti-Zr-Y (Pearce and Cann, 1973); A = island arc tholeiites, B = MORB, C = calc-alkaline basalts, D = within-plate basalts; (b) Hf-Th-Ta (Wood, 1979): A = N-MORB, B = E-MORB, C = alkaline within plate basalts; D = destructive plate margin basalts. Symbols as in Fig. 3.

MORB-normalized spiderdiagrams (Fig. 6a; Pearce, 1982) also show the typical pattern of the intraplate magmas, with enrichment in both LILE and HFSE. The shape of the diagram is, moreover, strikingly similar to that of P-type MORB of Wood et al. (1979). When normalized to primitive mantle (McDonough et al., 1992; not shown), the MM metabasites show patterns very similar to that of OIBs but with negative anomalies of K, Rb, Ba and Sr. Strong scattering of LILE may be related to element mobility during metamorphism, as also suggested by the high H_2O contents.

The REE patterns (Fig. 6b) for the MM samples exhibit a strong LREE enrichment (La_N/Yb_N = 6.3-11), particularly for the samples of the lower sub-unit, no negative Eu anomalies, or very slight positive ones for the samples of the upper sub-unit, and roughly flat HREE. Samples from the two upper sub-units also show the lowest LREE fractionation. A general increase in ΣREE with differentiation has been noticed.

The relatively narrow range of HFSE and the regularity and similarity of the REE patterns indicate that these elements have not been much affected by post-emplacement mobilisation and are expected to have retained the magmatic relationships of the protoliths (e.g Pearce and Cann, 1973; Floyd and Winchester, 1978; Floyd et al., 2000). Therefore, mostly HFSE and REE and their ratios have been used in order to obtain petrological information, mainly focused on petrogenetic processes and sources.

Sm-Nd isotopic data for two selected samples of MM metabasites are listed in Table 2 and plotted in the ε_{Nd}-Sm/Nd diagram (Fig. 7). ε_{Nd} values, recalculated at 480 Ma are + 3.92 and + 0.57 for the sample MM5 (lower sub-unit) and for the sample MM47 (upper sub-unit), respectively. The sample MM47 has higher Sm/Nd ratio than sample MM5.

DISCUSSION

Geochemical affinity and tectonic setting

In the Mongiuffi-Melia area, three discrete groups of metabasites can be recognized on the basis of geochemical data, which are consistent with the field and petrographical observations. In particular, samples from the lower sub-unit have a more alkalic nature with marked within-plate affinity whereas samples from the intermediate and upper sub-units have a more transitional character, with a P-MORB affinity.

REE patterns of MM metabasites are analogue to that of many Lower Palaeozoic meta-alkali basalts, e.g. the metabasites from the Apuan Alps (Conti et al., 1993) and northern Bohemian Massif (Floyd et al., 2000; Crowley et al., 2002, and references therein). They are also similar to patterns of modern transitional-mildly alkali basalts from the East African Rift (Wilson, 1989).

The ε_{Nd} values of the MM metabasites are very different from that typical of MORB-type basalts and are, on the contrary, analogue to that of the Lower Palaeozoic alkali metabasites linked to continental break-up from Massif Central

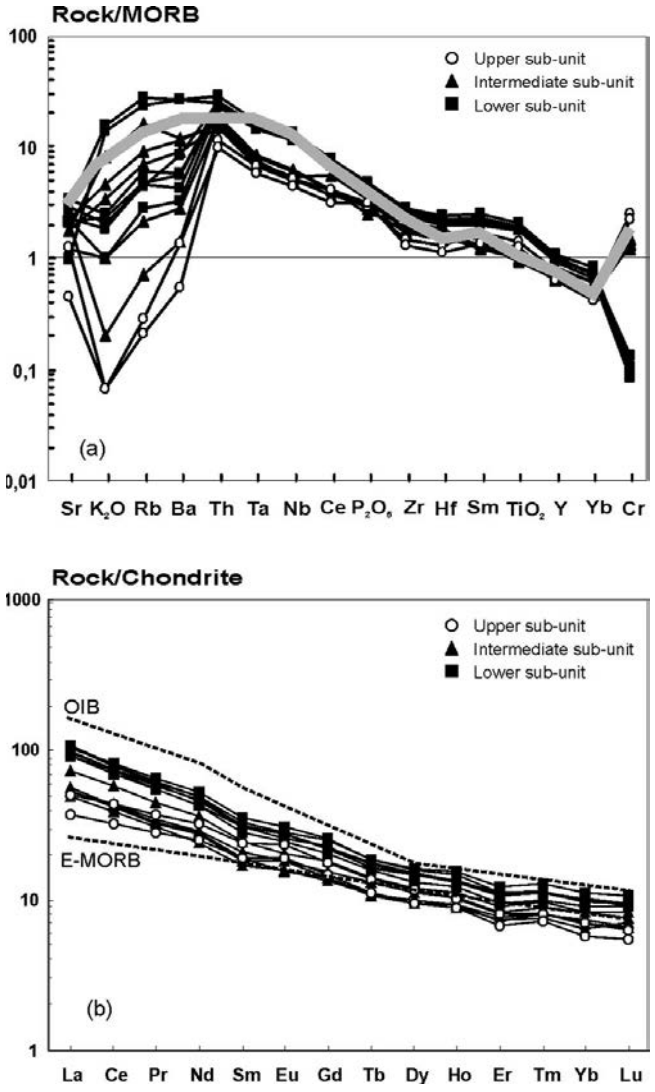

Fig. 6 - (a) Incompatible trace element pattern normalized to N-MORB (Pearce, 1982) for the MM metabasites. Superimposed line is the P-type MORB, after Wood et al. (1979); (b) REE patterns normalized to chondrites (Evensen et al., 1978); E-MORB and OIB compositon after Sun and McDonough (1989).

and NE Bohemian Massif, (e.g. Pin and Marini, 1993; Furnes et al., 1994; Patocka et al., 1997; Crowley et al., 2002). In the ε_{Nd}-Sm/Nd diagram (Fig. 7), sample MM5 plots indeed within the field of Western Sudetes Cambro-(?) to Ordovician alkaline metabasites that, as suggested by Furnes et al. (1994) and Crowley et al. (2002), represent an early stage of continental rifting. These alkaline metabasites are characterized by both lower ε_{Nd} and Sm/Nd values than other coeval metabasalts showing E-MORB to N-MORB affinity, respectively.

According to Furnes et al. (1994) the association of alkali basalts and MORB is the result of interaction of a plume-like component with the convecting asthenosphere in an extensional geodynamic setting.

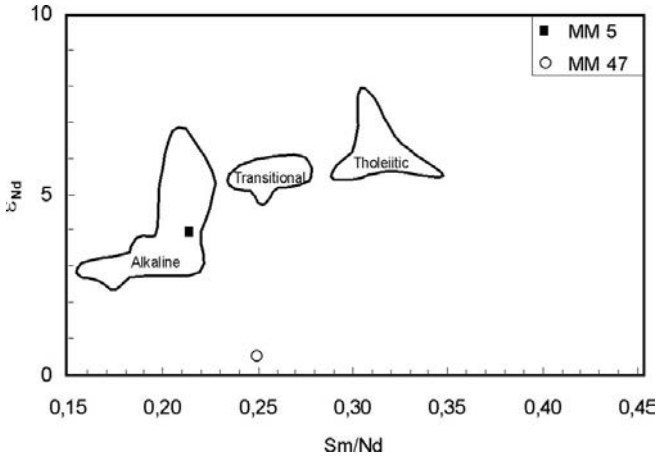

Fig. 7 - ε_{Nd} versus Sm/Nd diagram for the MM metabasites. Fields representative for composition of coeval alkali metabasites from NE Bohemian Massif are shown for comparison (reference data from Furnes et al., 1994; Crowley et al., 2002).

Role of fractional cystallization

The trends in the variation diagrams are consistent with the fractionation of olivine + clinopyroxene ± spinel, from the more primitive compositions of the upper sub-unit metabasites (picritic compositions for sample MM46) to the more evolved lower sub-unit rocks. The increasing abundance of Ti coupled with lack of overall decrease in Fe rule out any significant magnetite fractionation. Plagioclase fractionation probably did not play a significant role as inferred by the positive correlation between Al_2O_3 and Zr and the lack of Eu anomalies. Samples MM46 and MM47 from the upper sub-unit have high contents of Ni and Cr, which are indicative for equilibration of the original magmas with a peridotite mantle source.

The narrow variation of many incompatible element ratios and the sub-parallel REE-patterns of the MM metabasites may be interpreted in terms of both fractional crystallisation or variable degrees of partial melting of a single source. The metabasites from the three sub-units are characterised by different ranges of ratios as, for instance Zr/Nb (5.4-5.6 for lower samples; 8.6-9.1 for intermediate samples; 7.4-7.5 for upper samples), Nb/Y (1.3-1.4 for lower samples; 0.7-1.1 for intermediate samples; 0.8 for upper samples) and Zr/Y (7.3-8 for lower samples; 6.5-9.5 for intermediate samples; 5.7-6.1 for upper samples). These variations may be explained in terms of fractionation of clinopyroxene, in which Y behaves as compatible element and partition coefficient D_{Zr} is higher than D_{Nb}. Also the higher Sm/Nd ratio of the sample MM47, compared to that of the sample MM5, might be linked to the more primitive character of the former sample, since Sm/Nd ratio decreases with fractional crystallization.

Above data show that the geochemical features of the MM metabasites are consistent with an origin by fractional crystallization from a magma parent derived from a single mantle source. Nevertheless other processes might have operate producing analogue characteristics and some of the observed features result difficult to explain exclusively by fractional crystallization, as for example the relatively high value of the Th/Ta (2.33-2.42) and the low TiO_2 and Fe_2O_3 contents in the samples from the intermediate sub-unit. Different values of the element ratios may therefore indicate variable amounts of crustal contamination or occurrence of discrete partial melts from different sources in the generation of the different groups of metabasites.

Crustal contamination

The low ε_{Nd} values of sample MM47 should be justified invoking some extent of crustal contamination for these metabasites; crustal contamination has been actually claimed for Sudetic samples plotting in analogue position in the same diagram (Fig. 7; Furnes et al., 1994). The amount of contamination of ascending basaltic magmas by crustal components may be evaluated considering Th/Nb and La/Nb ratios (Pin and Marini, 1993). High Th/Nb ratios (0.11-0.18) of the MM metabasites may indeed represent for involvement of crustal components, such as the La/Nb ratios ≥ 1. In particular all but one of the metabasites from the two upper sub-units have La/Nb in the range 0.9-1.45. On the contrary, the samples from the lower sub-unit have La/Nb ratios of 0.83-0.93, falling in the range observed in strongly enriched ocean-island or "plume" basalts (P-MORB) (Pin and Marini, 1993, and reference therein).

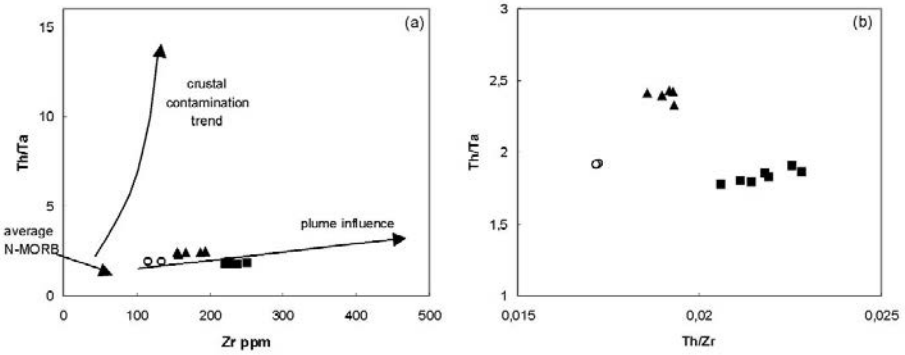

Fig. 8 - (a) Comparison of trends displayed by the MM metabasites in a Th/Ta vs. Zr diagram with trends of crustal contamination and plume influence displayed by rift-related basalts from North Atlantic continental margin (data from Thompson et al., 1982; 1986); (b) different trends displayed by the three groups of metabasites in a Th/Ta vs. Th/Zr diagram. Symbols as in Fig. 3.

Table 2 - Sm-Nd isotopic data for the selected MM metabasites

	Sm (ppm)	Nd (ppm)	Sm/Nd	$^{147}Sm/^{144}Nd$	$^{143}Nd/^{144}Nd$*	$^{143}Nd/^{144}Nd(t)$	εNd(t)
MM5	6.864	32.095	0.2139	0.1293	0.51263	0.51222	3.92
MM47	4.392	17.574	0.2499	0.1511	0.51252	0.51205	0.57

* measured ratio; initial $^{143}Nd/^{144}Nd$ ratio corrected for an assumed age of emplacement of 480 Ma

Data have been plotted in the Th/Ta vs. Zr diagram (Fig. 8a), together with the trends of crustal contamination and of plume influence on original N-MORB compositions (Thompson et al., 1982; 1986; Floyd et al., 2000). The MM metabasites clearly plot along the trend indicating plume influence (or fractionation influence), ruling out intensive crustal contamination. In particular only the samples from the upper sub-units are slightly displaced towards higher values of the Th/Ta ratio, so likely indicating some crustal contamination, just for the metabasites from these sub-units. The slightly different trends between the three sub-units are evidenced in the Th/Ta vs. Th/Zr diagram (Fig. 8b).

Source

The geochemical features of continental sodic alkali basalts are generally interpreted considering their parental magmas as the result of small degrees of melting (< 5% wt.) of active plume or of passively upwelling lithospheric or asthenospheric mantle. Decompression melting of sublithospheric mantle can be induced by lithospheric thinning particularly during the formation of continental rifts, the volumes of magmas depending on the thickness of the continental lithosphere and on the temperature of the sublithospheric mantle. In absence of important heat contributions (e.g. by mantle plumes), only small volumes of melt are generated and melting may be restricted to the stability field of garnet peridotite (Farmer, 2004). Melting of continental lithospheric mantle is hardly induced by simple litospheric thinning; it seems to require fluids and/or heat from the underlying mantle (Harry and Leeman, 1995).

Isotopic data provide important informations in order to distinguish basaltic magmas derived (partially at least) from the continental lithospheric mantle from that ones derived from the sublithospheric mantle. Normal continental lithospheric mantle (CLM) typically have lower ε_{Nd} (< 0) compared to sublithospheric mantle or metasomatized suprasubduction CLM (Farmer, 2004). Positive ε_{Nd} values of sodic alkali basalts such as that of MM metabasites**,** therefore suggest that their parental magmas were likely derived from variably enriched asthenospheric mantle sources. Nevertheless the isotopic data do not allow to exclude that these basalts were generated by melting of lithospheric mantle metasomatized just before melting, due to the introduction of incompatible element-rich fluids/melts derived from small degree melting of upwelling asthenosphere (Farmer, 2004). The MM metabasites are similar, in their ε_{Nd} and Sm/Nd values, to Cambro-Ordovician alkali metabasalts from the NE Bohemian Massif, French Massif and Iberian Massif which are thought to have originated from the North Gondwanan margin during an early episode of continental break-up (Pin and Marini, 1993; Furnes et al., 1994; Crowley et al., 2002). In such initial stage an enriched asthenosphere plume-like component was likely mainly involved in the process of magma generation.

The different degree of enrichment observed for trace elements from the different metabasite sub-units may be explained, in addition to fractionation processes, in terms of variable amount of mixing between asthenospheric N-MORB type depleted sources and OIB-plume enriched sources. In particular, the samples from the basal sub-unit show the highest amount of plume component. So, the temporal evolution of the basic magmatism could have involved increasing amount of a depleted source component.

In the Th/Yb vs. Ta/Yb diagram (Fig. 9; Pearce, 1982) the MM metabasites plot within the field representative for uncontaminated intraplate basalts derived from enriched mantle source. The slight displacement of the samples of the intermediate sub-unit towards relatively high Th/Yb ratios might indicate, consistently with the previous observations, some involvement of continental crust in their evolution.

As indicated by Crowley et al. (2000), basaltic rocks generated in evolving rift zones may display geochemical affinities with N-MORB, P-MORB and within plate basalts explainable in terms of source-related processes coupled with fractional crystallization and crustal contamination. In the Y/Nb vs. Zr/Nb diagram (Fig.10) data for MM metabasites are plotted together with the fields of Lower Palaeo-

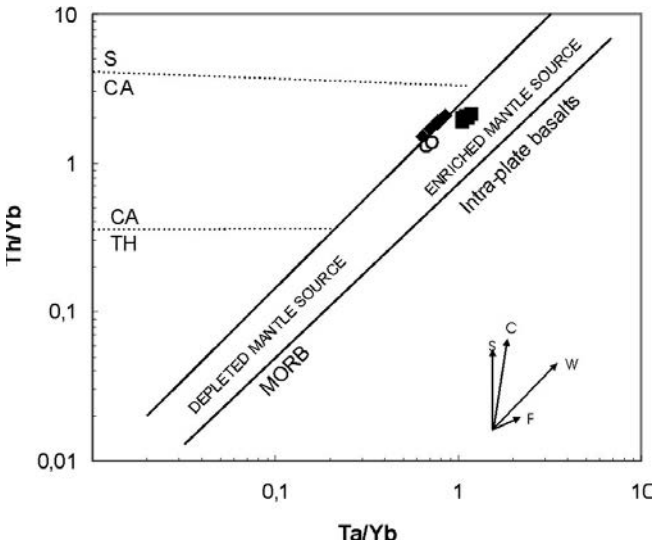

Fig. 9 - Composition of MM metabasites in the Th/Yb versus Ta/Yb diagram (Pearce, 1982). Vectors: S = subduction component, W = within plate enrichement, C = crustal contamination, F = fractional crystallization. Dotted lines separate the tholeiitic (TH), calc-alkaline (CA) and shoshonitic (S) fields. Symbols as in Fig. 3.

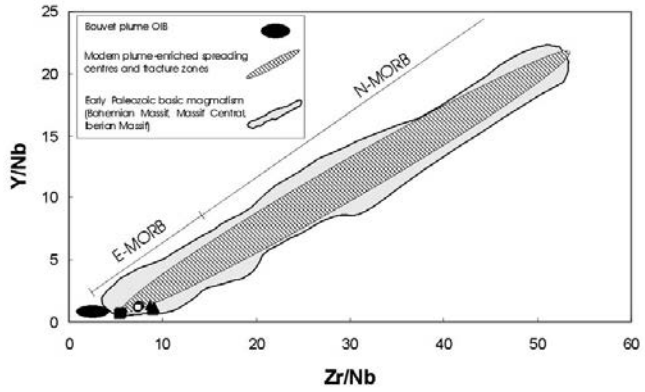

Fig. 10 - Comparison of composition of MM metabasites with Early Palaeozoic and modern basalts originated in extensional settings known to be influenced by upwelling mantle plumes (data from Crowley et al., 2000). Symbols as in Fig. 3.

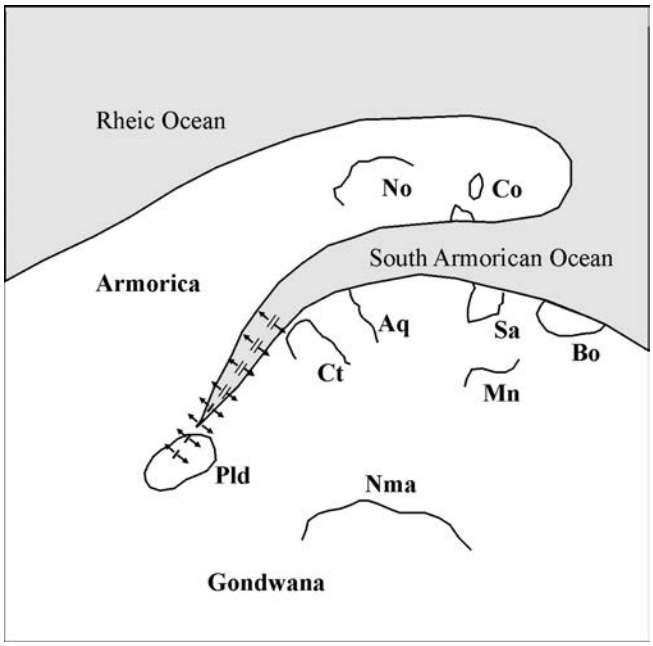

Fig. 11 - Simplified palaeogeographic reconstruction for peri-Gondwanan terranes in the Early Ordovician period (modified from Paris and Robardet, 1990; Carmignani et al., 1992; Atzori et al., 2001). Grey: oceanic crust; White: continental crust. No, Normandy; Co, Corsica and Northern Sardinia; Sa, central and southern Sardinia; Bo, Bohemia; Ct; Cantabria; Aq, Aquitania; Mn, Montagne Noire; Pld, Peloritan lower domain; Nma, Northern Maghreb.

zoic meta-basalts and younger American-Anctartic Ridge and Fracture Zone Basalts that are known to be influenced by an upwelling mantle plume (Crowley et al., 2000). By inspection of the diagram it is possible to infer for the MM metabasites a origin in an extensional setting influenced by upwelling plumes, as indicated for the Lower Palaeozoic metabasic rocks from Bohemian Massif, Massif Central and Iberian Massif (Crowley et al., 2000). In this diagram all the MM samples plot within the area representative for E-MORB and the less enriched nature of the metabasites from the two upper sub-units is again emphasized.

Finally, the Mongiuffi-Melia metabasites show low La/Nb and La/Ta ratios (generally < 1.2 and < 15.4, respectively) indicative of enriched asthenospheric sources rather than lithospheric sources which are, on the contrary characterised by La/Nb > 1.5 and La/Ta > 22 (Franceschelli et al., 2003, and references therein).

In summary, the geochemical features of Mongiuffi-Melia metabasites strongly argue for a within-plate to P-MORB affinity and derivation of the basaltic protoliths from variably enriched asthenospheric mantle sources with limited amount of crustal contamination during the ascent. Geochemical data are consistent with a geodynamic environment related to a continental rifting. In particular, the protoliths of studied rocks were most likely the result of an early stage of rifting involving passive rise of basaltic melts, without intervening of active upwelling plumes leading to extensive melting of the lithospheric mantle.

CONCLUSIVE REMARKS AND GEODYNAMIC IMPLICATIONS

The magmatic protoliths of Mongiuffi-Melia metabasites were emplaced during a Cambro-Ordovician magmatic event related to rifting preceding continental break-up. Magma generation was the result of decompression melting mainly induced by extensional tectonics. The basalts, characterized by within-plate to P-MORB affinity, were derived by a variably enriched asthenospheric mantle source and were only slightly modified by interaction with continental crust.

As a whole, the MM metabasites exhibit geochemical features comparable to those from the Apuan Alps (Conti et al., 1993), Sardinia (Ricci and Sabatini, 1978; Di Pisa et al., 1992) and other European terranes involved in the Lower Palaeozoic continental break-up (e.g. Pin and Marini, 1993; Crowley et al., 2000; 2002; Floyd et al., 2000). These results suggest that the Peloritani Lower Domain (Pld) was likely part of an “archipelago” of microcontinents separated by more or less developed seaways, only in some cases consisting of true oceanic basins. In particular, Peloritani Mountains represent a sector of the former Alboran microplate (Andrieux et al., 1971), also known as ALKAPECA (Alboran-Kabylie-Peloritan-Calabria; Bouillin et al., 1987), which is now fragmented within the Alpine belt of southern Europe and northern Africa. Alboran microplate is inferred to have occupied a central position within the peri-Gondwanan terranes originated by the Cambrian fragmentation of the northern margin of Gondwana. Nevertheless, some differences appear comparing the ages of magmatic products with similar affinity cropping out in different peri-Mediterranean areas. Clear diachronism exists, for example, between the continental rifting episode of Pld terrane, assigned to the Cambro-Ordovician and other peri-Gondwanan terranes, where true MORB rocks were generated at the same time. As proposed by von Raumer et al. (2003), different temporal evolution along the former Gondwana margin may indicate oblique processes of convergence and extension leading to generation of true oceanic crust only in separated pull-apart basins. According to these authors, the location of the oceanic basins was probably controlled by the stress applied at the plate boundaries during initial back-arc opening, although mantle plumes have probably contribute to rifting of the Rheic Ocean.

In such a Lower Ordovician scenario, location of the Pld terrane at the southwestern termination of the South Armorican Ocean, i.e. a branch of Rheic Ocean placed by Paris and Robardet (1990) between the Armorican and Gondwana plates (Fig. 11), appears consistent with the overall features of the MM metabasites. Such a location, tentatively proposed by Atzori et al. (2001), provides an appropriate explanation of both diachronism and limited amount of rift related magmatic products which did not evolve to formation of true oceanic crust.

Aknowledgements

The authors are thankful to J. Bébien, V. Bortolotti and an anonymous reviewer for their comments and suggestions which greatly improved the paper.

REFERENCES

Acquafredda P., Lorenzoni S. and Zanettin Lorenzoni E., 1994. Paleozoic sequences and evolution of the Calabrian-Peloritan Arc (Southern Italy). Terra Nova, 6: 582-594.

Andrieux J., Fontobé J.M. and Mattauer M., 1971. Sur un modèle explicatif de l'arc de Gibraltar. Earth. Planet. Sci. Lett., 12: 191-198.

Atzori P. and Ferla P., 1979. Caratteristiche del metamorfismo ercinico sulle successioni sedimentarie e magmatiche del basamento paleozoico delle unità inferiori dei M. Peloritani. Mem. Soc. Geol. It., 20: 447-452.

Atzori P., Cirrincione R., Del Moro A. and Pezzino A., 1994. Structural, metamorphic and geochronogical features of the Alpine events in the south-eastern sector of the Peloritani Mountains (Sicily). Per. Mineral., 63: 113-125.

Atzori P., Cirrincione R., Mazzoleni P., Pezzino A. and Trombetta A., 2001. A tentative pre-Variscan geodynamic model for the Palaeozoic basement of the Peloritani Mountains (Sicily): evidence from meta-igneous products. Per. Mineral., 70 (2): 255-267.

Bouillin J.P., Majesté-Menjoulas C., Baudelot S., Cygan C. and Fournier-Vinas C., 1987. Les formations paléozoiques de l'Arc Calabro-Peloritan dans leur cadre structural. Boll. Soc. Geol. It., 106: 683-698.

Capelli C., Cortesogno L. and Gaggero L., 1994. Metabasites and associates ultramafites in the cristalline basement of Ligurian Alps: petrochemical characterisation and geotectonic significance. Per. Mineral., 63: 179-197.

Carignan J., Hild P., Mevelle G., Morel J. and Yeghic Heyan D., 2001. Routine analyses of trace elements in geological samples using flow injection and low pressure on-line liquid chromatography coupled to ICP-MS: a study of reference materials BR, DR-N, UB-N, AN-G and GH. Geostandards Newsletter, 25 (2-3): 187-198.

Carmignani L., Barca S., Cappelli B., Di Pisa A., Gattiglio M., Oggiano G. and Pertusati P.C., 1992. A tentative geodynamic model for the Hercynian basement of Sardinia. IGCP 276, Newsletter, 5:61-82.

Cirrincione R., Atzori P. and Pezzino A., 1999. Sub-greenschist facies assemblages of metabasites from south-eastern Peloritani Range (NE Sicily). Mineral. Petrol., 67: 193-212.

Cirrincione R. and Pezzino A., 1994. Nuovi dati sulle successioni mesozoiche metamorfiche dei Monti Peloritani orientali. Boll. Soc. Geol. It., 113: 195-203.

Conti P., Di Pisa A., Gattiglio M. and Meccheri M., 1993. Prealpine basement in the Alpi Apuane (Northern Apennines, Italy). In: J.F. Von Raumer and F. Neubauer (Eds.), Pre-Mesozoic geology in the Alps. Springer Verlag, p. 609-621

Crowley Q.G., Floyd P.A., Winchester J.A., Franke W. and Holland J.G., 2000. Early Palaeozoic rift-related magmatism in Variscan Europe: fragmentation of the Armorican Terrane Assemblage. Terra Nova, 12: 171-180.

Crowley Q.G., Timmermann H., Noble S.R. and Grenville Holland J., 2002. Palaeozoic terrane amalgamation in Central Europe: a REE and isotopic Sm-Nd isotope study of the pre-Variscan basement, NE Bohemian Massif. In: J.A. Winchester, T.C. Pharaoh and J. Verniers (Eds.), Palaeozoic amalgamation of Central Europe. Geol. Soc. London Spec. Publ., 201: 157-176.

Di Pisa A., Gattiglio M. and Oggiano G., 1992. Pre-Hercynian magmatic activity in the Nappe zone (internal and external) of Sardinia: evidence of two within-plate basaltic cycles. In: L. Carmignani and F.P. Sassi (Eds.), Contributions to the geology of Italy with special regard to the Palaeozoic basement: A volume dedicated to Tommaso Cocozza. IGCP Project 276 Newsletter, 5: 107-116.

Evensen N.M., Hamilton P.J. and O'Nions R.K., 1978. Rare earth abundances in chondritic meteorites. Geoch. Cosm. Acta, 42: 1199-1212.

Farmer G.L., 2004. Continental basaltic rocks. In: H.D. Holland and K.K. Turekian (Eds.), Rudnick R. (Vol. Ed.), Treatise of geochemistry. Vol. 3: The crust, p. 85-116.

Ferla P., 1978. Natura e significato geodinamico del vulcanismo pre-ercinico presente nelle filladi e semiscisti dei Monti Peloritani (Sicilia). Rend. S.I.M.P, 34: 55-74

Floyd P.A. and Winchester J.A., 1978. Identification and discrimination of altered and metamorphosed volcanic rocks using immobile elements. Chem. Geol., 21: 291-306.

Floyd P.A., Winchester J.A., Seston R., Kryza R. and Crowley Q.G., 2000. Review of geochemical variations in Lower Palaeozoic metabasites from the NE Bohemian Massif: intracratonic rifting and plume-ridge interaction. In: W. Franke, R. Altherr, V. Haak, O. Oncken and D. Tanner (Eds), Orogenic processes - quantification and modelling in the Variscan Belt of Central Europe. Geol. Soc. London. Spec. Publ., 179: 155-174.

Franceschelli M. Cruciani G., Puxeddu M. and Utzeri D., 2003. Pre-Variscan metagabbro from NW Sardinia, Italy: evidence of an enriched asthenospheric mantle source for continental alkali basalts. Geol. J., 38: 145-159.

Furnes H., Kryza R., Muszynski A., Pin C. and Garmann L.B., 1994. Geochemical evidence for progressive, rift-related volcanism in eastern Sudetes. J. Soc. Geol. London, 151: 91-110.

Harry D.L. and Leeman W.P., 1995. Partial melting of melt metasomatized subcontinental magma and the magma source potential of the lower lithosphere. J. Geophys. Res., 100: 10255-10269.

Lentini F., Carbone S. and Catalano S., 1995. Principali lineamenti strutturali della Sicilia nord-orientale. Studi Geol. Camerti, Spec. Vol., p. 319-329.

Majesté-Menjoulas C., Bouillin J.P., Cygan C. and Fourmier Vinas C., 1986. Les formations paléozoïques (Cambrien à Carbonifère) des Monts Peloritans (Sicily). C. R. Acad. Sci. Paris, 303: 1315-1320.

McDonough W.F., Sun S., Ringwood A.E., Jagoutz E. and Hoffmann A.W., 1992. K, Rb and Cs in the Earth and Moon and the evolution of the Earth's mantle. Geoch. Cosmoch. Acta, Ross Taylor Symp. Vol., 56: 1001-1012.

Paris F. and Robardet M., 1990. Early Palaeozoic palaeobiogeography of the Variscan regions. Tectonophysics, 177: 193-213.

Patocka F., Dostal J. and Pin C., 1997. Early Palaeozoic intracontinental rifting in the central west Sudetes, Bohemian Massif: geochemical and Sr-Nd isotopic study on felsic-mafic metavolcanics of the Rychory Mts. Complex. Terra Nova (Abstr. Suppl.) 1: 144-145.

Pearce J.A., 1982. Trace elements characteristics of lavas from destructive plate boundaries. In: R.S. Thorpe (Ed.), Andesites: orogenic andesites and related rocks. Wiley, New York, p. 525-548.

Pearce J.A. and Cann J.R., 1973. Tectonic setting of basaltic volcanic rocks determined using trace element analyses. Earth. Planet. Sci. Lett., 19: 290-300.

Pezzino A., 1982. Confronti petrografici e strutturali tra i basamenti metamorfici delle unità inferiori dei Monti Peloritani (Sicilia). Per. Mineral., 1: 35-50.

Pin C. and Marini F., 1993. Early Ordovician continental break-up in Variscan Europe: Nd-Sr isotope and trace element evidence from bimodal igneous associations of the Southern Massif Central, France. Lithos, 29: 177-196.

Raumer J.F. von, Galetti G., Oberhänsli R. and Pfeifer H.R., 1990. Amphibolites from Lac d'Emosson/Aiguilles Rouges (Switzerland): tholeiitic basalts at a transition zone between continental and oceanic crust. Schweiz. Mineral. Petrog. Mitt., 70: 419-435.

Raumer J.F. von, Stampfli G.M., Borel G. and Bussy F., 2002. Or-

ganization of pre-Variscan basement areas at the north-Gondwanan margin. Int. J. Earth Sci., 91: 35-52.

Raumer J.F. von, Stampfli G.M. and Bussy F., 2003. Gondwana-derived microcontinents - the constituents of the Variscan and Alpine collisional orogens. Tectonophysics, 365: 7-22

Ricci C.A. and Sabatini G., 1978. Petrogenetic affinity and geodynamic significance of metabasic rocks from Sardinia, Corsica and Provence. N. Jb. Miner. Monatsh., (1): 28-38

Schaltegger U., Gebauer D. and Quadt A. von, 2002. The mafic-ultramafic rock association of Loderio-Biasca (lower Pennine nappes, Ticino, Switzerland): Cambrian oceanic magmatism and its bearing on early Palaeozoic paleogeography. Chem. Geol., 186: 265-279.

Shervais J.W., 1982. Ti-V plots and the petrogenesis of modern and ophiolitic lavas. Earth. Planet. Sci. Lett., 59: 101-118.

Stampfli G.M. and Borel G.D., 2002. A plate tectonic model for the Palaeozoic and Mesozoic constrained by dynamic plate boundaries and restored synthetic oceanic isochrons. Earth. Planet. Sci. Lett., 196: 17-33.

Sun S.S. and McDonough M.F., 1989. Chemical and isotopic systematics of oceanic basalts: implications for mantle composition and processes. In: A.D. Saunders and M.J. Norry (Eds.), Magmatism in oceanic basins. Geol. Soc. London. Spec. Publ., 42: 313-345.

Thompson R.N., Dickin A.P., Gibson I.L. and Morrison M.A., 1982. Elemental fingerprints of isotopic contamination of Hebridean Palaeocene mantle-derived magmas by Archean sial. Contrib. Miner. Petrol., 79: 159-168.

Thompson R.N., Morrison M.A, Dickin A.P., Gibson I.L. and Harmon R.S., 1986. Two contrasting styles of interaction between basic magma and continental crust in the British Tertiary Volcanic province. J. Geoph. Res., 91: 985-5997.

Wilson M., 1989. Igneous petrogenesis. Unwin Hyman, London, 465 pp.

Wood D.A., Tarney J., Varet J., Saunders A.D., Bougault H., Joron T., Treuil M. and Cann J.R., 1979. Geochemistry of basalts drilled in the North Atlantique by IPOD 49: implication for mantle heterogeneity. Earth. Planet. Sci. Lett., 42: 77-97.

Received, January 12, 2005
Accepted, June 3, 2005